

Evidence of Kramer extrapolation inaccuracy for predicting high field Nb₃Sn properties

Christopher Segal^{1,2}, Christian Barth², Iole Falorio², Alejandro Carlón Zurita², Amalia Ballarino², Xavier Chaud³, Chiara Tarantini¹, Peter J. Lee¹, and David C. Larbalestier¹

¹ASC-NHMFL, Florida State University, Tallahassee, U.S.A

²CERN, Geneva, Switzerland

³LNCMI, Grenoble, France

Christopher.Brian.Segal@cern.ch

Abstract. Future applications requiring high magnetic fields, such as the proposed Future Circular Collider, demand a substantially higher critical current density, J_c , at fields ≥ 16 T than is presently available in any commercial strand, so there is a strong effort to develop new routes to higher J_c Nb₃Sn. As a consequence, evaluating the irreversibility field (H_{irr}) of any new conductor to ensure reliable performance at these higher magnetic fields becomes essential. To predict the irreversibility field for Nb₃Sn wires, critical current measurements, I_c , are commonly performed in the 12-15 T range and the Kramer extrapolation is used to predict higher field properties. The Kramer extrapolation typically models the contribution only for sparse grain boundary pinning, yet Nb₃Sn wires rely on a high density of grain boundaries to provide the flux pinning that enables their high critical current density. However, whole-field range VSM measurements up to 30 T recently showed for Nb₃Sn RRP[®] wires that the field dependence of the pinning force curve significantly deviates from the typical grain boundary shape, leading to a 1-2 T overestimation of H_{irr} when extrapolated from the typical mid-field data taken only up to about 15 T. In this work we characterized a variety of both RRP[®] and PIT Nb₃Sn wires by transport measurements up to 29 T at the Laboratoire National des Champs Magnétiques Intenses (LNCMI), part of the European Magnetic Field Laboratory in Grenoble, to verify whether or not such overestimation is related to the measurement technique and whether or not it is a common feature across different designs. Indeed we also found that when measured in transport the 12-15 T Kramer extrapolation overestimates the actual H_{irr} in both types of conductor with an inaccuracy of up to 1.6 T, confirming that high field characterization is a necessary tool to evaluate the actual high field performance of each Nb₃Sn wire.

1. Introduction

The 100 TeV Future Circular Collider (FCC) envisioned at CERN will require a large number of Nb₃Sn bending magnets which will need to operate in the 16 T range [1,2]. Currently, only two wire manufacturing processes have demonstrated the potential to bring Nb₃Sn into this high field operation range: the Rod Restack Process (RRP[®]) produced by Bruker OST [3], and the Powder In Tube (PIT) technique produced by Bruker EAS [4–6]. Despite recent efforts to further optimize the existing



chemistry, architecture and heat treatment of these conductors, the J_c appears to be limited well below the desired $1,500 \text{ A/mm}^2$ (16 T, 4.2 K) demanded for FCC [7]. In an effort to push Nb_3Sn superconducting technology to its limits, the conductor community has been focussing R&D towards the introduction of additional pinning centers (APC) to increase J_c in the superconducting transport layer, and also to shift the maximum of the pinning force curve to higher fields. Currently there are multiple groups working on variants of the PIT process to introduce additional pinning centers. Fermilab and Ohio State University, in collaboration with Hyper Tech Research, Inc, reintroduced the previously developed internal oxidation technique, in which Nb1Zr is oxidized at final wire size to form ZrO_2 precipitates that both increase grain boundary density and provide additional pinning centres [8]. However, the need to supply oxygen to the Nb_3Sn during reaction increases the complexity of production especially if non-PIT routes are considered. At the Applied Superconductivity Center (ASC), part of the National High Magnetic Field Laboratory in Tallahassee, Florida, significantly refined Nb_3Sn grains were produced without using oxygen by adding Hf to the standard Nb4at%Ta alloy. In studies comparing Nb4Ta, Nb4Ta1Zr and Nb4Ta1Hf with and without a SnO_2 source, the highest J_c , well above the FCC specification, was found in a SnO_2 -free wire of Nb4Ta1Hf. This surprising result appears to have its basis in the delaying of recrystallization of pure Nb or Nb4Ta which occurs during the A15 reaction above $600 \text{ }^\circ\text{C}$. With Hf (or Zr) present in the alloy, the density of grain boundary diffusion paths of Sn into the alloy is greatly increased and maintained during the A15 reaction, allowing a much finer A15 grain size [9].

The impact of these new approaches on the properties at magnetic fields $\geq 16 \text{ T}$ is not yet fully understood and even the properties of conventional strands are seldom characterized beyond 16 T as such fields are not typically available outside the national high field laboratories. Thus it is valuable to make measurements from low to very high field that can then be used to model the field versus current behaviour over a broad range, enabling more reliable predictions based on measurements from more accessible lower field magnets ($< 15 \text{ T}$). The common approach to characterizing wires for high field applications has been to use transport J_c data measured in the 12-15 T range, then extrapolate using the Kramer expression [10] to predict the irreversibility field (H_{irr}) where the flux lines become fully depinned and J_c goes to zero. Thus H_{irr} is approximated as the Kramer field H_k , where the Kramer function (eq 1) goes to zero.

$$f_k(\mu_0 H) = [J_c(\mu_0 H)]^{0.5} \cdot (\mu_0 H)^{0.25} \quad (1)$$

This Kramer model takes into account only the contribution of sparse grain boundary pinning, consistent with the relatively low grain boundary density of 100-200 nm diameter grains. However, there are signs from recent measurements on the highest critical current density production wires (Bruker-OST RRP®) that the Kramer function can deviate from linearity making extrapolations from low or mid-fields inadequate for predictions of the high-field performance [11]. Moreover, the newer Zr or Hf wire designs can have significant point pinning as well as significantly denser grain boundary pinning due to their $< 100 \text{ nm}$ grain diameters. They might thus be expected to further deviate from linearity, driving the need for a more appropriate extrapolation methods, as has recently been discussed [11].

2. Experimental Details

High field measurements were performed using the 29 T high field resistive magnet at the Laboratoire National des Champs Magnétiques Intenses (LNCMI) in Grenoble, France. The LNCMI is one of three laboratories forming the European High Magnetic Field Laboratory (EMFL). This 24 MW resistive magnet has a 50 mm bore diameter (38 mm diameter cryostat) and field homogeneity of 860 ppm in a 1 cm sphere at the center.

We used a probe (supplied by the LNCMI) typically used for ReBCO tape measurements that simply terminates with two rectangular copper rods to which a sample holder is attached. As the cryostat diameter limits straight sample lengths to $< 38 \text{ mm}$, we preferred to prepare our Nb_3Sn wire

samples on VAMAS (Versailles Project on Advanced Materials and Standards) barrels in order to characterize longer lengths.

The VAMAS barrels are made of Ti-6Al-4V alloy which has a similar thermal expansion coefficient as Nb₃Sn [12], and are grooved to better support the strand. A thin ceramic layer is baked onto the barrel to prevent sticking of the wire and allow easy removal after measurement, allowing the barrels to be reused. Cu rings were then attached to the top and bottom of the VAMAS barrel, and the strand wound onto the barrel with the ends of the strands fixed to the Cu caps by soldering after heat treatment. Two pairs of voltage taps were then added; the first set measures voltage across the inner 6 turns (~60 cm), while the second set is attached to the Cu end caps and measures voltage across the entire length of the conductor (~90 cm). The last step is to apply vacuum grease across the barrel to provide some support during measurement at cryogenic temperatures. The barrelled samples were mounted on the measurement probe such that the Lorentz force generated when injecting current is inward, thus providing support by the barrel. A typical sample mounted on the VAMAS barrel and ready for measurements is shown in figure 1.



Figure 1. The bottom image shows our VAMAS adapter with a sample mounted before attaching to the measurement probe, shown at the top.

The main advantage of VAMAS barrels over straight samples is that ~1 m of wire is used, and we can reliably measure the voltage across the inner 60 cm, 60 times the length of short samples where we typically measure the voltage over only 1 cm. It was, however, necessary to develop an adaptor which could hold a VAMAS barrel and connect to the LNCMI probe.

The most challenging aspect of designing this adaptor was that the as-prepared VAMAS barrels are ~32 mm in diameter with too little space between the barrel and the cryostat wall to run current leads around to the lower end of the barrel, thus requiring the current to be routed through the centre of the barrel. This demanded some complex geometries and, although we considered using a 3D printed Cu adaptor, the final piece was classically machined from OFE Cu with RRR ~300.

For data processing we used a custom analysis script, executed in the IGOR software from WaveMetrics [13]. The software takes the raw data from the inner voltage taps as input, then removes any offset and resistive slope: the corrected I-V curves are fitted with the typical power law function. I_c is then determined from the fitting curve using the electric field of criterion 0.1 $\mu\text{V}/\text{cm}$. In a few

cases where the typical I-V characteristic was not obtained due to wire instability at low field and high current, the quench current was assumed to be I_c .

2.1. Samples measured

We measured five different Nb₃Sn wires, three PIT and two RRP (table 1). All three PIT samples are from the last generation of high-field conductors manufactured by Bruker EAS. They are Ta doped, 192 filament wires, 0.85 mm diameter and utilize a Nb bundle barrier that allows for a more aggressive reaction without degradation of RRR [14]. Of the three PIT conductors, wire 62902 (referring to billet number) was reacted with a typical heat treatment of 415°C/40 h + 620°C/120 h + 645°C/200h, and wire 51603 was reacted using an inverted multistage heat treatment (IMHT) of 660°C/10h + 620°C/120h + 640°C/120h. This type of heat treatment (HT) has the benefit of a much improved small to large grain Nb₃Sn ratio [6], as well as a higher temperature reaction stage which usually improves the high field properties [15]. Further details on the motivation for using an IMHT are described in [6]. We additionally measured another 51603 wire which was similarly heat treated but rolled to 15% deformation to simulate cabling deformation [14] and to investigate the effect of diffusion barrier breach and Sn leaking into the Cu [16] on the high field performance. Billets 62902 and 51603 are nominally the same. The RRP conductors have a 108/127 architecture with Ti doping. They were heat treated at 210°C/48h + 400°C/48h + 650°C/50h for the 0.7 mm diameter wire, and 210°C/48h + 400°C/48h + 665°C/50h for the 0.85 mm wire.

Table 1: Heat treatment details of Nb₃Sn samples measured in high magnetic field at LNCMI.

Wire type	Billet	Deformation%	Wire diameter (mm)	Heat Treatment	Dopant
PIT	62902	0%	0.85	415/40+620/120+645/200 (standard HT)	Ta
PIT	51603	0%	0.85	660/10+620/120+640/120 (IMHT)	Ta
PIT	51603	15%	0.85	660/10+620/120+640/120 (IMHT)	Ta
RRP	00019	0%	0.70	210/48+400/48+650/50	Ti
RRP	00385	0%	0.85	210/48+400/48+665/50	Ti

3. Results and analysis

We measured the five Nb₃Sn barrels at increasing fields from 10 T to the irreversibility field (25-26 T), defined as the field where the I-V curve shows only a resistive transition and there is no visible loss-free curve below the voltage criterion of 0.1 μ V/cm. All measurements are self-field corrected as described in [17]. An example of the raw I-V curves at the highest fields near H_{irr} are shown in figure 2. After correcting for resistive offset, fitting the data to reduce noise, and applying the self-field corrections, we can determine the non-Cu critical current density (J_c) for an applied magnetic field. In figure 3, this field dependence of the J_c is shown for all five samples over the entire field range. As previously described, the data in figure 3 can then be linearized using the Kramer function (eq.1) and its extrapolation to zero is thought to provide an approximation for the magnetic field ($\mu_0 H_k$) where J_c goes to zero, marking H_{irr} , the physical irreversibility field [10]. An example for the 0.85 mm RRP wire is shown in figure 4.

To improve the accuracy of the true H_{irr} values reported here, we considered the highest field where we saw little or no signal in the superconducting state, and also considered extrapolating the highest field measurements to further refine the H_{irr} value. For example, the 25.5 T curve in figure 2 shows that the wire begins its resistive transition below one amp, so we know the H_{irr} would be higher than 25.5 but lower than 26 T. To reduce this half Tesla uncertainty window, an extrapolation over the highest field data just below H_{irr} (24, 24.5, 25, 25.5 T) can be performed. For this wire we arrived at an H_{irr} of 25.8 T; 1.6 T below the 27.4 T predicted by the Kramer extrapolation from the typical 12-15 T range. It is seen in figure 4 that the extrapolation from 20 T upwards is in close agreement with the reported H_{irr} , within 0.4 T in all cases (table 2). Since this manuscript focuses on the relative error of the predicted field rather than the absolute value, we normalized the extrapolated Kramer field (H_k) to

the measured irreversibility field (H_{irr}) and plot that value against the highest field in the extrapolated field range, starting extrapolations at 12 T (figure 5a). For example, the point at (~ 19 , 0.98) uses the data from 12-19 T, and predicts an H_{irr} 98% of the true value. All three PIT wires and the 0.85 mm RRP wire show over-predicted H_k values, while the 0.7 mm RRP shows a slight under-prediction. In figure 5b, the confidence interval from the extrapolations is shown to demonstrate variation in uncertainty depending on the field ranges that are used.

Only extrapolating up to 15 T can over-predict H_{irr} by 6% with confidence intervals exceeding 0.5 T. Including additional higher field measurements in the extrapolations show that closer to H_{irr} the over-prediction is $< 3\%$ with the confidence interval dropping to about 0.2 T. As a matter of completeness, the PIT standard sample has no point at 15 T as we were unable to measure at 12 T, and the few points produce an unrealistically large confidence interval.

While the Kramer expression does approximately linearize the data, we found that f_k over-predicts H_{irr} by up to 1.6 T when using the typical 12-15 T range for the extrapolation (see table 2). The actual irreversibility field, H_{irr} , and extrapolations, H_k , from different ranges are shown in table 2 for all wires.

The round PIT wire with a standard HT and the 0.85 mm RRP wire had the highest H_{irr} at 26.1 and 25.8 T, respectively. The 0.7 mm RRP wire had the lowest H_{irr} of 24.9 T (however, we note that its

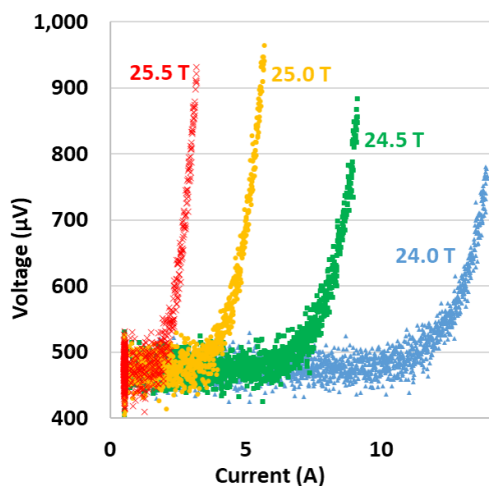


Figure 2: Raw I-V curves for RRP 0.85 mm wire from 24-25.5 T. Despite the $\sim 100 \mu\text{V}$ noise, the resistive transitions are clearly seen.

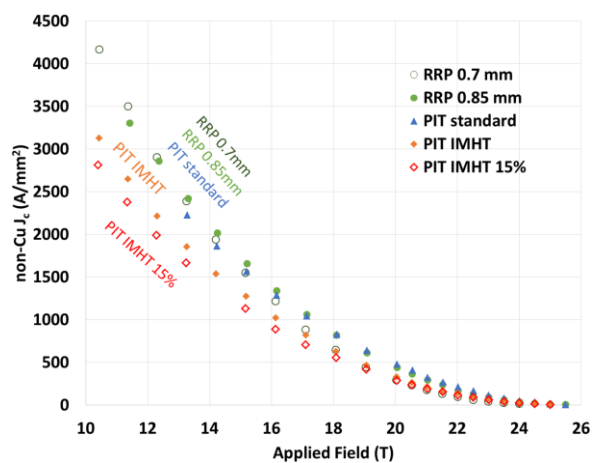


Figure 3: J_c dependence on applied magnetic field for all samples. All PIT wires are 0.85 mm diameter.

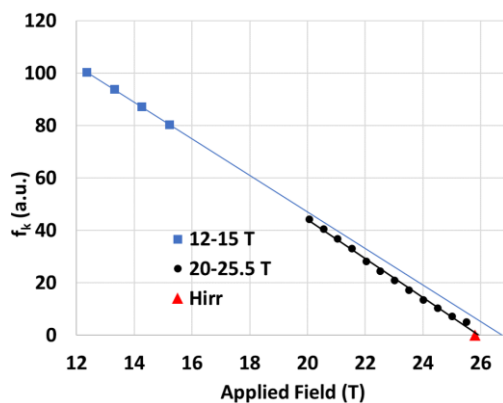


Figure 4: Kramer plot of mid-field and high-field extrapolations. The legend indicates the field ranges of the different extrapolations.

Table 2: Measured H_{irr} values compared to H_k extrapolations from different field ranges. The extrapolation in the typical 12-15 T range shows an over prediction of H_{irr} by up to 1.5 T. Extrapolation from fields above 20 T are much closer to the true value.

	Measured $\mu_0 H_{irr}$	$\mu_0 H_k$ different ranges	
		12-15 T	20 T- H_{irr}
PIT standard	26.1	27.7	26.3
PIT IMHT	25.5	26.6	25.7
PIT IMHT 15%	25.5	26.4	25.9
RRP 0.7	24.9	24.7	25.1
RRP 0.85	25.8	26.8	25.9

HT is 15°C lower than for the 0.85 mm RRP wire). The PIT wires which underwent the IMHT, both round and rolled, had H_{irr} of 25.5 T, about 0.5 T less than the PIT wire with the recommended standard HT.

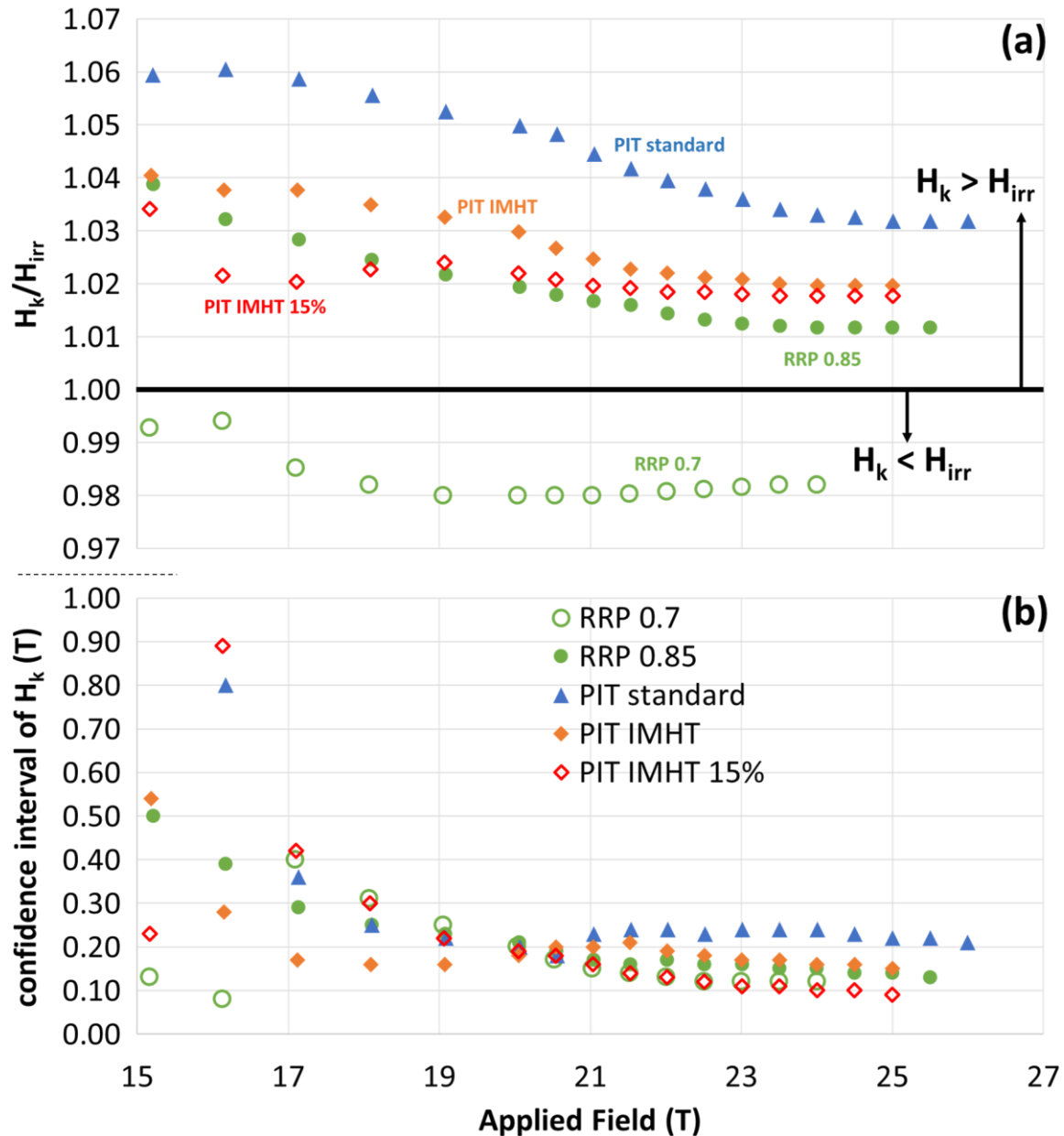


Figure 5: In plot (a) we normalized the extrapolated Kramer field (H_k) to the measured irreversibility field (H_{irr}) and plotted this value against the highest field in the extrapolated field range, starting at 12 T. For example, the point at (~19, 0.98) uses the data from 12-19 T, and predicts an H_{irr} 98% of the true value. The 0.85 mm wires all have over predicted H_k values, while the 0.7 mm is slightly under predicted. In (b), the confidence interval from the extrapolations is shown. The PIT standard sample has no point at 15 T as we were unable to measure at 12 T, and the few points produce an unrealistically large confidence interval. It can be seen that the confidence interval falls to ~0.2 T by 20 T for all samples.

4. Discussion

For many years, Nb₃Sn wires have been characterized by measuring J_c from 12 to 15 T using the Kramer extrapolation to predict the irreversibility field. There is a well-developed correlation between higher J_c at 12-15 T and higher H_{irr} . As we are considering Nb₃Sn for magnets operating at up to about 20 T, it is important to know the true high field properties to fully understand their operating margins. To this end it was recently found by Tarantini *et al.* [11] that this commonly used mid-field Kramer extrapolation consistently over predicts H_{irr} by more than 2 T using Vibrating Sample Magnetometry (VSM) up to 30 T. The data reported here confirms these earlier VSM conclusions that H_{irr} cannot be reliably predicted using Kramer extrapolations from 12-15 T for RRP wires and also demonstrates that the same issue exists for PIT conductors (figure 5). We also demonstrate that this inaccuracy is not dependent on the measurement technique, as both transport and VSM show similar overestimations. Using different field ranges above 15 T for the extrapolation can reduce this inaccuracy to only ~0.5 T. However, this requires access to magnets generating more than 15 T, which are not commonly available for such measurements.

We also validated here that the 0.7 mm RRP wire has almost 1 T lower H_{irr} than the 0.85 mm RRP wire, likely impacted by the 15 °C lower HT temperature as lower reaction temperatures have been shown to produce lower H_{irr} values [18]. Additionally, this wires Kramer extrapolation was the only to under predict its H_{irr} , though more measurements are required to properly interpret this result.

This set of PIT samples also allowed us to study how the new IMHT would affect H_{irr} , and if rolled wires had different high field performance than round wires. Despite the degradation in J_c , produced by rolling, the PIT IMHT wires had the same H_{irr} for both round and rolled samples. This suggests that the initial part of the small grain A15 layer which forms before the Sn leaks out maintains a high Sn content in these wires, even in filaments which are compromised from rolling. Additionally, the Sn-poor Nb₃Sn which forms towards the end of the reaction likely only contributes to transport current at lower fields.

The overall 0.6 T reduction of H_{irr} from the typical HT to the IMHT may be due to a reduced amount of Sn in the Nb₃Sn layer. In fact, the high temperature stage seems to cause a higher A15 phase nucleation rate which generates a thicker small grain A15 layer. However, the overall Sn content of the A15 layer may be lower, suppressing H_{irr} . Further analysis to determine the composition of the Nb₃Sn layer by EDS mapping will be performed to verify this hypothesis.

Additionally, there is commonly known to be slight curvature in the Kramer extrapolation depending on the field range [19][20], however, we found it difficult to resolve with our 0.5 T steps. We will determine if these wires do show similar behaviour during future measurements.

5. Conclusions

The Kramer extrapolation of measurements in the mid-field range from 12-15 T has been widely used to predict the irreversibility field of Nb₃Sn wires. The high field transport measurements presented here show that the Kramer extrapolation typically overestimates H_{irr} by up to 1.6 T for PIT and RRP wires reacted with various heat treatments. Although there are ongoing efforts to determine a reliable extrapolation method, our results suggest that the only way to reliably determine H_{irr} of these conductors is to measure transport current until H_{irr} is reached. Additionally, our investigation reveals that, although the inverted multistage heat treatment forms more Nb₃Sn [6,21], this is accomplished by negatively affecting J_c and H_{irr} . On the other hand the rolled PIT conductor shows lower J_c than its round equivalent but maintains an identical H_{irr} . The causes of these behaviours require further investigations.

Acknowledgements

We are very grateful to our colleagues in the TE/MS-SCD section at CERN: Marina Malabaila, Konstantina Konstantopoulou, Pierre-Francois Jacquot, Adrian Szeliga, Angelo Bonasio, Hasan Ayhan, and Simon Hopkins. This work was supported by the US Department of Energy (DOE) Office of High Energy Physics under award DE-SC001208, the National High Magnetic Field Laboratory (which is supported by the National Science Foundation under NSF/DMR-1644779), the State of

Florida, and CERN under grants KE1920/TE and RF02226. We also acknowledge the support of the LNCMI-CNRS, member of the European Magnetic Field Laboratory (EMFL).

References

- [1] Ballarino A, et al. 2019 The CERN FCC Conductor Development Program: A Worldwide Effort for the Future Generation of High-Field Magnets *IEEE Trans. on App. Supercon.* **29** 1–9
- [2] Tommasini D, et al. 2017 The 16 T Dipole Development Program for FCC *IEEE Trans. on App. Supercon.* **27** 1–5
- [3] Sanabria C, Field M, Lee P J, Miao H, Parrell J and Larbalestier D C 2018 Controlling Cu–Sn mixing so as to enable higher critical current densities in RRP[®] Nb₃Sn wires *Supercond. Sci. Technol.* **31** 064001
- [4] Tarantini C, Segal C, Sung Z H, Lee P J, Oberli L, Ballarino A, Bottura L and Larbalestier D C 2015 Composition and connectivity variability of the A15 phase in PIT Nb₃Sn wires *Supercond. Sci. Technol.* **28** 095001
- [5] Segal C, et al. 2016 Evaluation of critical current density and residual resistance ratio limits in powder in tube Nb₃Sn conductors *Supercond. Sci. Technol.* **29** 085003
- [6] Segal C, Tarantini C, Lee P J and Larbalestier D C 2017 Improvement of small to large grain A15 ratio in Nb₃Sn PIT wires by inverted multistage heat treatments *IOP Conf. Ser.: Mater. Sci. Eng.* **279** 012019
- [7] Ballarino A and Bottura L 2015 Targets for R&D on Nb₃Sn Conductor for High Energy Physics *IEEE Trans. on App. Supercon.* **25** 1–6
- [8] Xu X, Sumption M D and Peng X 2015 Internally Oxidized Nb₃Sn Strands with Fine Grain Size and High Critical Current Density *Adv. Mat.* **27** 1346–50
- [9] Balachandran S, Tarantini C, Lee P J, Kametani F, Su Y-F, Walker B, Starch W L and Larbalestier D C 2019 Beneficial influence of Hf and Zr additions to Nb_{4at%}Ta on the vortex pinning of Nb₃Sn with and without an O source *Supercond. Sci. Technol.* **32** 044006
- [10] Kramer E J 1973 Scaling laws for flux pinning in hard superconductors *J. Appl. Phys.* **44** 1360–70
- [11] Tarantini C, Balachandran S, Heald S M, Lee P J, Paudel N, Choi E S, Starch W L and Larbalestier D C 2019 Ta, Ti and Hf effects on Nb₃Sn high-field performance: temperature-dependent dopant occupancy and failure of Kramer extrapolation *Supercond. Sci. Technol.*, vol. **32**, no. 12, p. 124003, Nov. 2019
- [12] Thilly L, Scheuerlein C, Stuhr U, Bordini B and Seeber B 2009 Residual Strain in a Nb₃Sn Strand Mounted on a Barrel for Critical Current Measurements *IEEE Trans. on App. Supercon.* **19** 2645–8
- [13] *IGOR Pro* (Software) (*Wavemetrics, Lake Oswego, OR, USA*)
- [14] Bordini B, Ballarino A, Macchini M, Richter D, Sailer B, Thoener M and Schlenga K Jun. 2017 The Bundle-Barrier PIT Wire Developed for the HiLumi LHC Project *IEEE Trans. on App. Supercon.*, vol. **27**, no. 4, pp. 1–6
- [15] Fischer C M, Lee P J and Larbalestier D C 2002 Irreversibility field and critical current density as a function of heat treatment time and temperature for a pure niobium powder-in-tube Nb₃Sn conductor *AIP Conf. Proc.* **614** 1008–15
- [16] Brown M, Tarantini C, Starch W, Oates W, Lee P J and Larbalestier D C 2016 Correlation of filament distortion and RRR degradation in drawn and rolled PIT and RRP Nb₃Sn wires *Supercond. Sci. Technol.* **29** 084008
- [17] Bordini B 2010 Self-field correction in critical current measurements of superconducting wires tested on ITER VAMAS barrels, CERN Internal Note, EDMS Nr: 1105765
- [18] Tarantini C, Lee P J, Craig N, Ghosh A and Larbalestier D C 2014 Examination of the trade-off between intrinsic and extrinsic properties in the optimization of a modern internal tin Nb₃Sn conductor *Supercond. Sci. Technol.* **27** 065013
- [19] Uglietti D, Seeber B, Abächerli V, Cantoni M and Flükiger R 2006 Strain and Field Scaling Laws for Internal Sn and Bronze Route Nb₃Sn Wires up to 21 T *AIP Conf. Proc.* **824** 528

- [20] Godeke A, Jewell M C, Fischer C M, Squitieri A A, Lee P J and Larbalestier D C 2005 The upper critical field of filamentary Nb₃Sn conductors *Journal of Applied Physics* **97** 093909
- [21] Segal C 2018 Performance limits of Powder in Tube Processed Nb₃Sn Superconducting wires *Florida State University (Thesis)*